行政院國家科學委員會專題研究計畫 成果報告

有機光電流增益現象之探討與其在光偵測器的應用
研究成果報告(精簡版)

中 華 民 國 100 年 10 月 27 日

一、報告內容

（一）前言

光偵測器可吸收光能轉並轉換成電訊號，利用電訊號即可偵測光源訊號的強弱。傳統的半導體光偵測器多數使用矽或化合物無機半導體為主動材料。而近來已有越來越多的研究投入於有機光偵測器。相較於無機材料，多數有機材料有較低的折射率(refraction index)，因此容易導入(coupling)光子於元件之中[1]；有機材料也有可撓性，且其重量輕、容易攜帶，並且製程溫度低，可製作於可撓性塑膠基板上，因此易於與其它的有機電子光電元件整合，例如有機光學積體電路(organic photonic integrated circuit)等[1]。

有機光偵測器除了可用於一般的光偵測應用之外，目前也有些研究單位提出幾種特殊且有趣的應用。例如日本東京大學 T. Someya 等人，將有機光偵測器與有機電晶體結合後，發展出可撓的影像掃描器(sheet image scanner)[2,3]，此裝置不但輕薄且可應用於大面積彎取平面的影像擷取。而在 2008 年，S. R. Forrest 的團隊也利用了有機光偵測器的可撓性，製作出半圓共焦平面陣列(hemispherical focal plane array)的偵測器[4]。不同於數位相機中高光圈數(f/number)且複雜的光學物件，此有機光偵測器陣列如同人眼一樣，可以很輕易地實現低光圈數且非常寬之場視野(field of view)，更重要的是，這是一般光偵測器不容易達成的目標。此研究對發展電子眼(electronic-eye cameras)是非常重要的發展[4]。

有機光偵測器研究領域中，近來有越來越多的研究探討光子增益(photomultiplication)現象。然而目前文獻上對於有機紅外光偵測器及有機材料中的光子增益現象的機制探討相對來說仍非常稀少，因此無論是在理論上或是實驗證據上仍有非常大的發展空間，這些知識也對未來發展高效率的有機光電元件乃至於相關的應用也將有重要的影響，因此我們必須重視此研究課題，並進一步有系統地研究。

（二）研究目的

從目前有機光偵測器的發展來看，還有兩大問題仍有待解決，第一、光偵測器的敏感度仍有進步的空間。第二、對於一般常用的有機半導體而言，其吸收大多還是在可見光範圍，應用範圍畢竟較為狹小。因此若光偵測器能偵測到較寬廣的波長範圍，如近紅外光等，其相對於可見光而言，具有低色射(dispersion)還有低損耗(lose)，可偵測的範圍也會比較大，可應用於光學通訊、光學斷層攝影(optical tomography)、監視器、夜視(night version)等。本計劃研究目的即是為了解決這些問題，我們將利用光子增益現象大幅提升元件效率，同時深入探討藉由摻雜(dope)方式達成高分子光偵測器中光子增益現象之機制，並改善元件特性，並研究元件效能的提升與改善之相關物理機制。

（三）文獻探討

有機光偵測器元件原理如圖一所示[5]，當光子被有機材料吸收後產生電子電洞對(hole-electron pair)或是可稱之為激子(exciton)，當激子飄移到 p 型材料 (donor)及 n 型材料 (acceptor)的接面時，由於 p 型材料具有較低的游離能，n 型材料具有較高的電子親和力，使得激子可以藉由此能量差而分離為自由電荷，電子再經由 n 型材料傳輸到陰極被收集，而電洞載子則經由 p 型材料傳輸被陽極所收集，最後形成光電流。
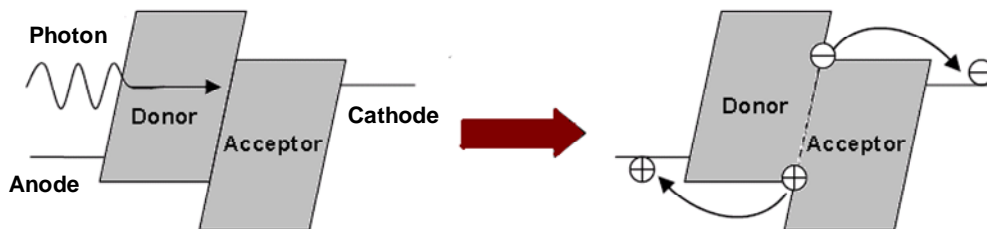
圖一、有機光偵測器元件結構跟原理之簡易示意圖[5]。

最早有機光偵測器元件由單層的高分子所組成[6]，但是一般激子於有機半導體中的束縛能(binding energy)很大，不容易分離，若沒有上述的 PN 接面，多數激子將再結合(recombination)而喪失能量，因此單層元件的效率並不好，其敏感度(sensitivity)只有 9×10^{-12} A/W。然而在 1994 年，A. J. Heeger 等人在高分子材料中加入 C_{60} 之後，發現可以大幅增加其敏感度，如圖二所示，有機光偵測器的敏感度在可見光區可與一般市售的 Si 光偵測器相比擬，而在 UV 區域更是有更高的敏感度[7]，因此更是適合在 UV 區域的應用。
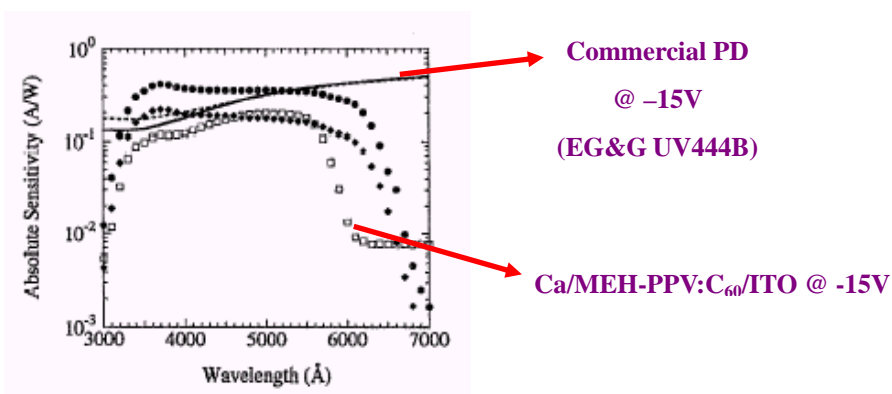

圖二、有機太陽能光偵測器對光波長的敏感度，並與市售之 Si 偵測器作比較[7]。

利用相同的概念，陸陸續續也有不少的相關論文發表，例如在以小分子有機物製作偵測器元件的研究方面，相較於高分子，小分子有機物的優點在於較易製作多層元件，因此 P. Peumans 等人的團隊在 2000 年，利用多層結構，製作出高頻寬(bandwidth)的光偵測器[8]。在 2005 年 H. W. Lin 等人也利用小分子化合物製作紫外光區域的偵測器，此元件的特色則在於對可見光是不靈敏的(visible-blind) [9]。

近幾年來，有更多重要的有機光偵測器相關研究發表，例如 Y. Yao 等人在 2007 年利用低能間隙的高分子，發表了近紅外光的偵測器[10]。2009 年，M. S. Arnold 等人則在 Nano. Letter 發表了使用有機半導體及奈米碳管達成廣泛光譜範圍(400~1450 nm)的光偵測器製作[11]。同年，T. Rauch 等人則在 Nature Photonics 發表了使用高分子及 PdS 奈米粒子製作近紅外光的偵測器，並結合矽背版(backplanes) 製成近紅外光的影像感測器[12]。

在 2008 年，H. Y. Chen 等人於 *Nature Nanotechnology* 中發表了一篇關於光子增益 (Photomultiplication)現象的論文[13]。作法是把 CdTe 奈米粒子溶於有機溶劑中，然後利用摻雜的方式使之與高分子 P3HT 及 C_{60} 衍生物 PCBM 混合,在低操作電壓下即可達到高光電導增益(Photoconduction gain),如圖五所示,在-5V 的逆向偏壓下,元件具有相當大的光電流,而其量子轉換效率(EQE)在 350nm 時,可高達 8000%；在 750nm 時也可超過 100%。換言之,具有光子增益的現象,可達到非常高的敏

感度。而如圖三(b)，光偵測器也有很寬廣的波長偵測範圍。在光子增益元件的操作機制方面，作者的推論如下：圖三(a)之插圖為元件的能階圖，由圖可知當光吸收後產生激子，在 P3HT 與 PCBM 接面分離成電子及電洞後，電子會被限制在錦化鎘奈米粒子中，因此當大量的電子推積於元件中時，產生強大的電場，使得在逆向偏壓的條件下，原本電洞注入的能障大幅降低，而有多餘的電洞可以大量的注入元件當中。
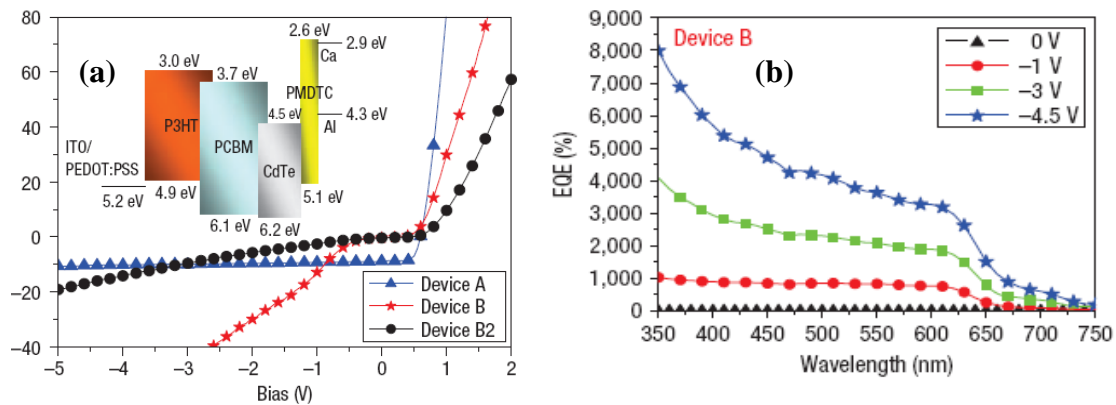
圖三、(a)元件的能階圖以及在逆向偏壓下之電性圖，A 元件經溶劑退火之製程且無摻雜奈米粒子，B 則摻雜了 CdTe 奈米粒子，B2 則摻雜了 CdTe 奈米粒子但未經溶劑退火之製程。(b)在逆向偏壓下，不同波長之 EQE。在 350nm 下，EQE 約 8000%[13]。

　　若上述 H. Y. Chen 等人推測的機制是正確的，產生光子增益現象的重點在於必須於元件中引入電荷捕陷(trap)，因此摻雜物(dopant)理論上不一定是要 CdTe 奈米粒子。緣此，不同於上述摻雜無機奈米粒子的方式，本計畫將利用摻雜**有機染料分子**的方式製作具有光子增益現象的高分子光偵測器，並利用此一系統深入地探討有機物質的光子增益現象，並改善元件特性。此外，值得注意的是在本計畫中，我們不使用無機奈米粒子而改用**有機染料分子**為摻雜物，其原因主要有三：第一、目前已有許多長波長的有機染料分子可供選擇，不但選擇較無機材料多，其多樣化的化學結構有利於未來機制的研究。第二、從以往的研究經驗來看，有機無機混成的元件多數有相分離的問題要考量，雖然使用有機染料分子不表示沒有相分離的現象，但預計相分離的問題程度會較低，元件效能會較高。第三、有機分子相較於多數的半導體無機奈米粒子具有較低的毒性，較符合目前綠色(green)研究的潮流。

　　(四)研究方法

元件製作：

　　圖四(a)為有機材料的結構式；圖四(d)則為元件的結構圖，首先我們將鍍有透明導電電極ITO的玻璃經過超音波震盪器搭配有機溶劑清洗，接著經過長時間100度以上的烘乾，之後將導電高分子材料 PEDOT:PSS 以旋轉塗佈的方式於乾淨的 ITO 玻璃基板上，在烤乾之後，以有機溶劑 1,2-dichlorobenzene(DCB) 混合有機主動層材料 P3HT/PCBM [poly(3-hexylthiophene)/ [6,6]-phenyl C61-butyric acid methyl ester]，以旋轉塗佈的方式沉積P3HT/PCBM 混合的薄膜，此外我們同時將有機染料分子摻雜物加入主動層內部；之後將基板移入熱蒸鍍機中蒸鍍金屬，即完成元件的製作。

　　(五)結果與討論

a. 摻雜有機染料分子導致光子增益現象：

　　圖四為P3HT及PCBM、有機染料分子IR-125及三者混合物的吸收光譜，從圖中可看出IR-125從600

3

至1100 nm有強烈的吸收，所以當P3HT及PCBM主動層摻雜IR-125後，吸收光譜可以延伸至約1100 nm。圖五為元件的特性圖，從圖中可以明顯看出當主動層摻雜IR-125後，光電流大幅地增加。而從量子轉換效率EQE曲線看來[圖五(b)]，在非常低壓的逆向偏壓-1.5V的條件下，最高量子轉換效率在510nm可高達7200%；同時在550nm時，偵測響應度(responsivity)最高可達32.4A/W；而在近紅外光區域如800nm，EQE也可達757%，這些數據確實證實使用有機染料分子可達到光子增益的現象。此外，圖五(b)的插圖為標準元件(未加入IR-125)的外部量子轉換效率，可看出量子效率隨著偏壓的上升並沒有太大的改變，均維持大約在50%~60%附近，因此可證明加入有機染料分子是元件光子增益的關鍵所在。元件的能階圖如圖四(b)所示，明顯指出屬於電子載子捕捉的元件，當元件吸收光子並產生電子電洞分離之後，在逆向偏壓的條件下，電洞可順利流出元件，但電子將被捕捉在位能井內，因此當大量的電子推積於元件中時，產生強大的電場，使得在逆向偏壓的條件下，原本電洞注入的位能障大幅降低，而有多餘的電洞可以大量的注入元件當中，最後被電極接收產生大量的電流值，獲得所謂的光電增益效應。
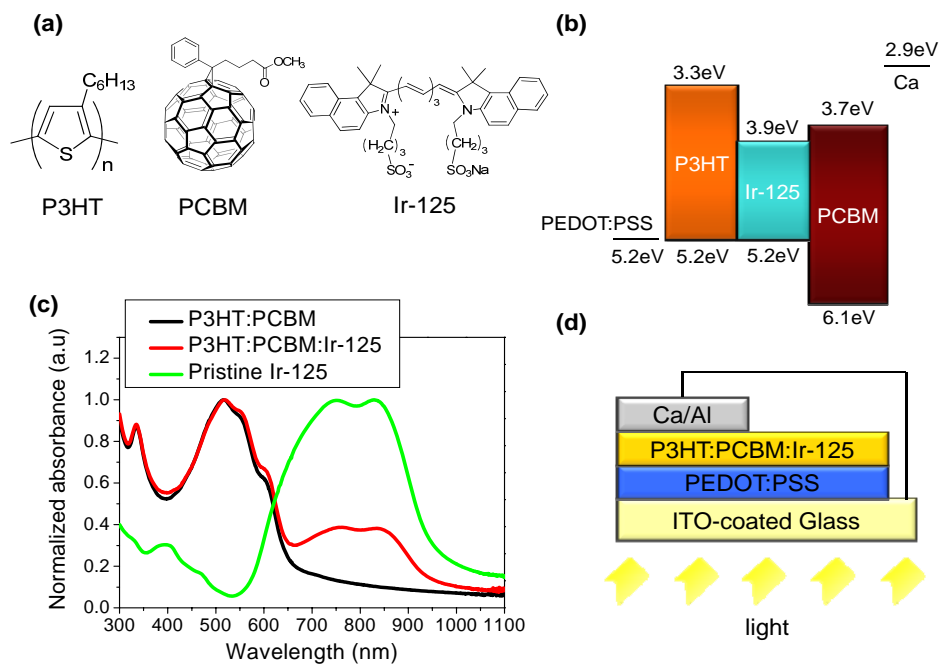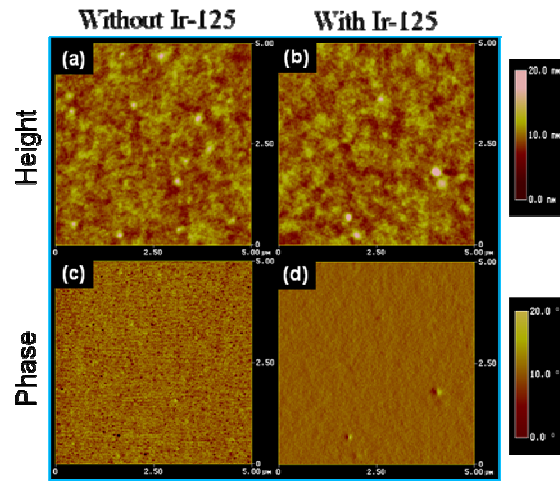

圖四、(a)有機材料的結構式；(b)元件的能階圖；(c)材料的吸收光譜；(d)則為元件的結構圖。
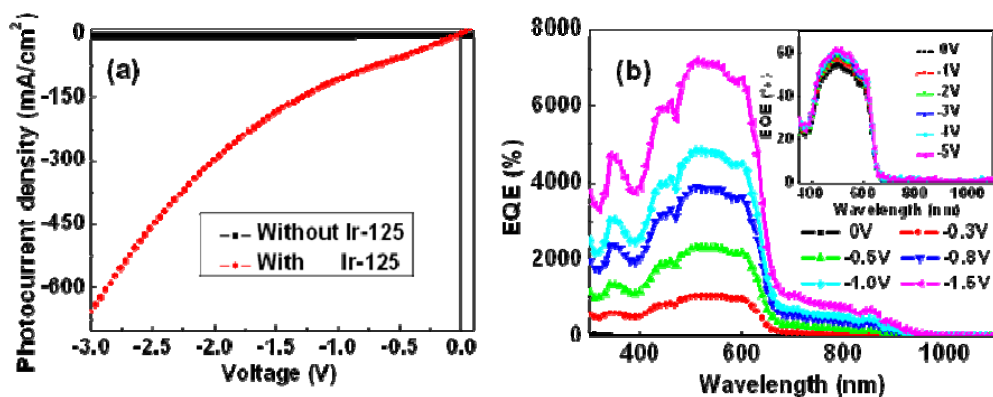
圖五、(a)元件加入Ir-125前後在AM1.5G 的太陽模擬光(100 mWcm^{-2})照射下的光電流電壓曲線；(b)元件在不同逆向偏壓下的外部量子轉換效率。插圖則為標準元件的外部量子轉換效率。

圖六為主動層加入 Ir-125 前後的表面形貌，圖六(a)及(b)的表面粗糙度(roughness)分別為 1.215 及

1.336 nm，顯示 Ir-125 的加入對表面形貌並沒有太多的影響，圖六(c)及(d)的相差模式(phase-mode)圖也有類似的結果，因此我們推測 Ir-125 應很均勻的分佈於薄膜中，而能有效的捕捉電子。

圖六、元件薄膜在加入Ir-125前[圖(a)及(c)]後[圖(b)及(d)]的表面形貌。其中圖(a)及(b)為高度差模式(height-mode)圖；圖(c)及(d)為相差模式(phase-mode)圖。

b. 雙重摻雜物以延伸波長偵測範圍

　　為了進一步延伸可偵測的波長範圍，我們嘗試兩種染料分子，除了前述之 Ir-125 之外，我們也加入 Q switch 1[圖七(b)]，從圖七(a)的吸收光譜圖中可看出 Q switch 從 900 至 1300 nm 有強烈的吸收，所以當於 P3HT 及 PCBM 主動層摻雜 IR-125 及 Q-switch 後，吸收光譜可以延伸至約 1300 nm。
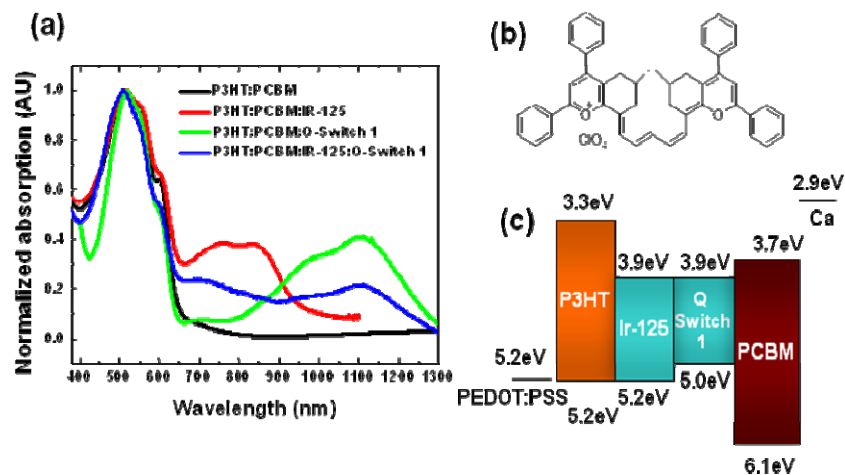
圖七、(a)材料的吸收光譜; (b)Q switch 1的化學結構式; (c)元件的能階圖。

　　圖八(a)為元件中只含有Q switch 1的量子轉換效率EQE曲線，雖然仍可觀察到光子增益的現象，但可明顯看出當量子轉換效率相對來說較低。從元件的能階圖[圖七(c)]可看出，Q switch 1可以補捉電子，但也可以捕抓電洞，因此我們推測較低的EQE可能是因為電子與電洞之間的遷移率相差較小，因此降低了光子增益的強度。但有趣的是元件若同時加入IR-125與Q switch 1，我們又可以得到很明顯的光子增益[圖八(b)]，同時因為有兩種摻雜物，光子增益現象的波長範圍可以延伸到~1200 nm。整體元件的光偵測範圍可從400 nm~1200 nm!我們推測加入Ir-125後，因有更強的電子補捉能力，因此可增強元件光子增益的效果。
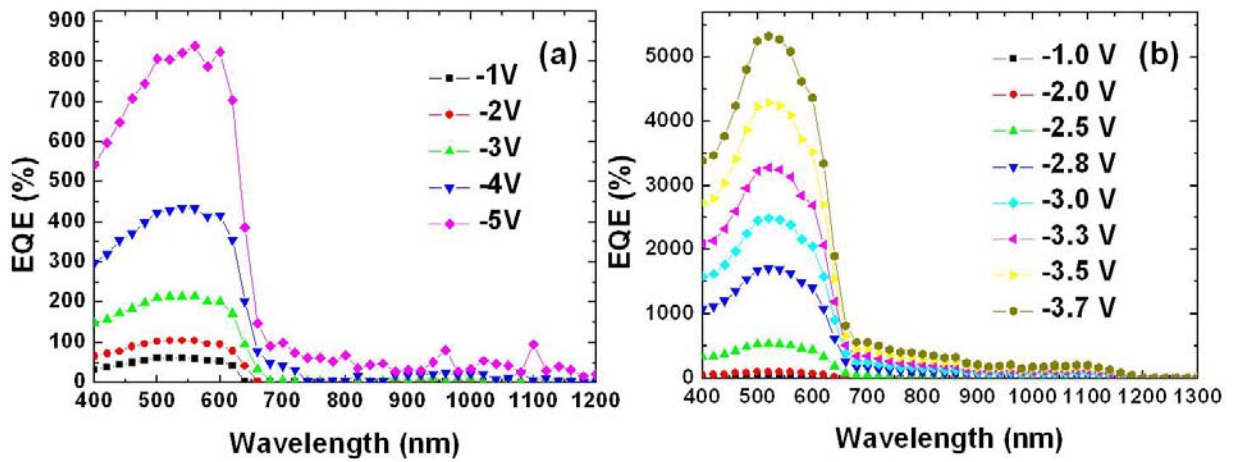
圖八、(a)元件單加入Q switch 1在不同逆向偏壓下的外部量子轉換效率；(b)同時加入Ir-125及Q switch 1在不同逆向偏壓下的外部量子轉換效率。

c. 元件暗電流的抑制

　　雖然我們已得到不錯的光電流，但我們也發現加入Ir-125分子後，元件的暗電流也同時增加了，將影響偵測度(detectivity)的提升，因此為了降低元件的暗電流，我們進一步在有機主動層之上利用熱蒸鍍的方式加上一層電荷阻擋層(charge blocking layer)，因Ir-125在元件中捕捉電子載子，因此電荷阻擋層選擇使用2,9-dimethyl- 4,7-diphenyl-1,10-phenanthroline (BCP)。整個元件的能階圖也如圖九(a)所示。圖九(b)加入不同厚度BCP後的暗電流，可以很明顯地看出，BCP確實可以有效地降低元件之暗電流。從圖中的能階圖可看出，在逆偏壓時電洞有機會注入P3HT或Ir-125的最高佔有分子軌域(highest occupied molecular orbital, HOMO)，加入BCP後，推測可以大縛降低電洞之注入。此外也可能可以降低電子注入元件後被收集的機率，而降低整體元件的暗電流。
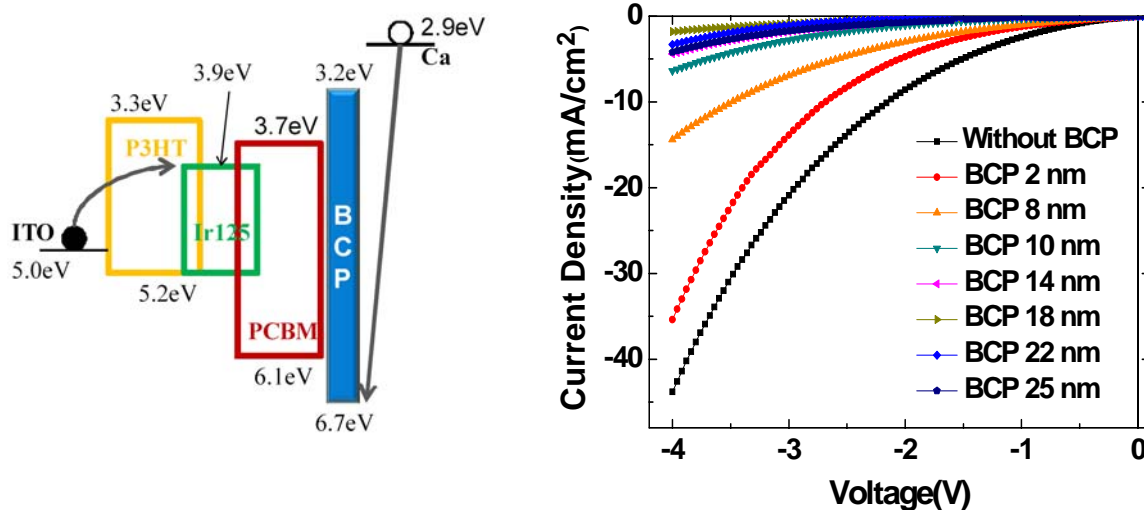
圖九、(a)元件的能階圖與機制示意圖；(b)不同BCP厚度元件在暗室下的電流密度-電壓特性。

　　圖十(a)為元件在逆向偏壓-0.20V下元件的外部量子轉換效率，可看到當BCP厚度為22nm時，元件最高外部量子轉換效率可達~2000%。對於一個光偵測器而言，雖然於學理上外部量子轉換效率(EQE)是個很重要的指標，而在實際應用上另一個重要的指標則為偵測度(detectivity)。偵測度之定

義為：

$$D^* = \frac{(A\Delta f)^{0.5}}{NEP} \quad (1)$$

其中A為元件偵測面積，單位為cm^2；Δf為頻寬，單位為Hz；NEP為雜訊等效功率(Noise equivalent power)，當光打在偵測器上所形成的電流訊號中，包含了一些雜訊，這些雜訊來自於暗電流 (Dark current)、約翰遜雜訊 (Johnson noise) 和熱擾動雜訊 (Thermal fluctuation noise or flicker noise)，一般來說暗電流為最主要的雜訊來源，因此NEP可表示為：

$$NEP = \frac{i_n}{R} \quad , i_n = (2q\ I_d \Delta f) \quad (2)$$

其中i_n即為雜訊訊號強度，R為光響應度(Responsivity)，將公式(2)代入公式(1)即可得到：

$$D^* = \frac{(A\Delta f)^{0.5}R}{i_n} = \frac{R}{(2qJ_d)^{0.5}}$$

式中R的單位為A/W、J_d的單位為$A\ cm^{-2}$，因此D^*的單位為$Hz^{0.5}\ cm/W$，又1 Jones = $Hz^{0.5}\ cm/W$。由此公式得知若能同時降低元件暗電流以及提升元件光電流，則光偵測元件的偵測度將會大幅提升。
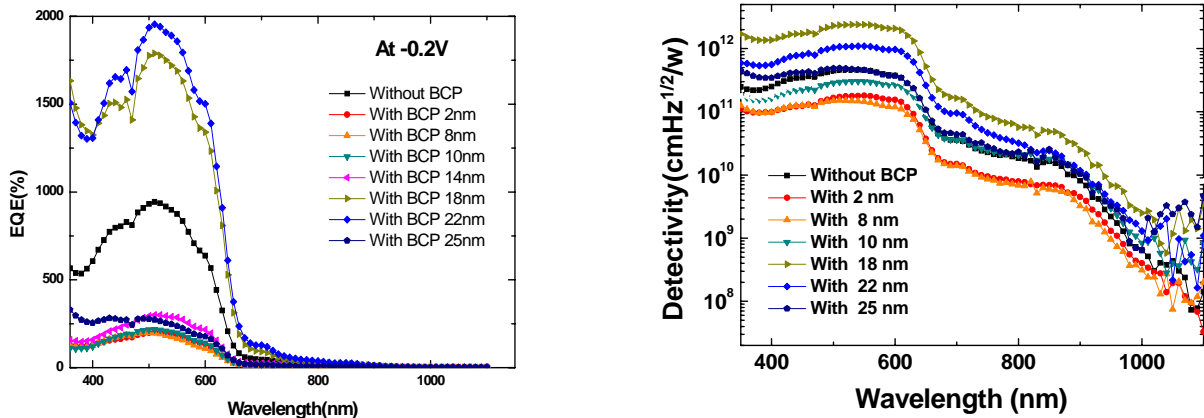
圖十、(a)在逆向偏壓-0.20V下，不同BCP厚度元件的外部量子轉換效率。(b) 不同BCP厚度元件不同波長的偵測度。

根據以上公式之推導，我們可求出元件在不同波長下的偵測度[圖十(b)]，可看出當 BCP 厚度為 18 nm 時，元件於波長為 550nm 之處的偵測度為 2.4×10^{12} Jones (1 Jones = $Hz^{0.5}$ cm/W)，相較於未加 BCP 的元件時的偵測度(4.5×10^{11} Jones)有極為明顯的提升。此結果充份顯示出電荷阻擋層能改善有機光偵測器的光偵測度。

在這個計畫的執行內容中，我們在主動層摻雜有機染料分子後，可觀察到明顯的光電增益效應。我們也發現藉由不同的有機染料分子摻雜，可以延伸元件可以偵測的波長。最後，我們也成功利用電荷阻擋層降低元件暗電流，能改善有機光偵測器的光偵測度。

參考文獻

1. P. Peumans, V. Bulović, and S. R. Forrest, *Appl. Phys. Lett.,* **76**, 3856 (2000).
2. T. Someya, Y. Kato, S. Iba, Y. Noguchi, T. Sekitani, H. Kawaguchi, and T. Sakurai, *IEEE Trans. Elec. Dev.*, **52**, 2502 (2005).
3. http://www.ntech.t.u-tokyo.ac.jp/index.html
4. X. Xu, M. Davanco, X. Qi, and S. R. Forrest, *Org. Electron.*, **9**, 1122 (2008).
5. P. Peumans, A. Yakimov, and S. R. Forrest, *J. Appl. Phys.* **93**, 3693 (2003).
6. G. Yu, C. Zhang, and A. J. Heeger, *Appl. Phys. Lett.*, **64**, 1540 (1994).
7. G. Yu, K. Pakbaz, and A. J. Heeger, *Appl. Phys. Lett.*, **64**, 3422 (1994).
8. P. Peumans, V. Bulović, and S. R. Forrest, *Appl. Phys. Lett.,* **76**, 3856 (2000).
9. W. H. Lin, S. Y. Ku, H. C. Su, C. W. Huang, Y. T. Lin, K. T. Wong, and C. C. Wu, *Adv. Mater.*, **17**, 2489 (2005).
10. Y. Yao, Y. Liang, V. Shrotriya, S. Xiao, L. Yu, and Y. Yang, *Adv. Funct. Mat.*, **19**, 3979 (2007).
11. M. S. Arnold, J. D. Zimmerman, C. K. Renshaw, X. Xu, R. R. Luny, C. M. Austin, and S. R. Forrest, *Nano Lett.* **9**, 3354 (2009).
12. T. Rauch, M. Böberl, S. F. Tedde, J. Fürst, M. V. Kovalenko, Günter, U. Lemmer, W. Heiss and O. Hayden, *Nature Photonics.* **3**, 332 (2009).
13. H. Y. Chen, M. K. F. Lo, G. Yang, H. G. Monbouquette, and Y. Yang, *Nature Nanotech.* **3**, 543 (2008).

已發表之期刊論文 (謝誌中有本計劃之編號)

1. Jyh-Lih Wu, Fang-Chung Chen,* Ming-Kai Chuang and Kim-Shih Tan "Near-infrared laser-driven polymer photovoltaic devices and their biomedical applications" **Energy Environ. Sci.**, 4, 3374 (2011). **(IF: 9.446)** (highlighted by a feature article in the *Chemistry World,* a monthly magazine published by Royal Society of Chemistry, July 2011; selected as "Hot Article" in Energy Environ. Sci. Blog)

2. Fang-Chung Chen,* Ming-Kai Chuang, Shang-Chieh Chien, Jheng-Hao Fang, and Chih-Wei Chu "Flexible polymer solar cells prepared using hard stamps for the direct transfer printing of polymer blends with self-organized interfaces" **J. Mat. Chem.** 21, 11378 (2011) **(IF: 5.099)**

3. Fang-Chung Chen*, Yung-Shiuan Chen, Shang-Chieh Chien, Cheng-Hsiang Liao and Shao-Tang Chuang "Suppression of phase separation through blending of electron transporting materials in polymer electrophosphorescent devices" **J. Lumin.** 131, 565 (2011) **(IF:1.795)**

4. Jyh-Lih Wu, Fang-Chung Chen*, Yu-Sheng Hsiao, Fan-Ching Chien, Peilin Chen, Chun-Hong Kuo, Michael H. Huang, and Chain-Shu Hsu "Surface plasmonic effects of metallic nanoparticles on the performance of polymer bulk-heterojunction solar cells" **ACS Nano** 5, 959 (2011) **(Times Cited:5) (IF:9.855)**

5. Fang-Chung Chen*, Tzung-Da Chen, Bing-Ruei Zeng and Ya-Wei Chung "Influence of mechanical strain on the electrical properties of flexible organic thin-film transistors" **Semicond. Sci. Tech.** 26, 034005 (2011) **(Times Cited:1) (IF:1.323) (invited paper)**

6. Fang-Chung Chen*, Shang-Chieh Chien, and Guan-Lin Cious "Highly sensitive, low-voltage, organic photomultiple photodetectors exhibiting broadband response**" Appl. Phys. Lett.** 97, 103301 (2010) **(Times Cited:1) (IF:3.820)**

計畫成果自評部份：

　　本計畫已成功證明在主動層摻雜有機染料分子後，可得到明顯的光電增益效應。我們也發現藉由不同的有機染料分子摻雜，可以延伸元件可以偵測的波長。最後，我們也成功利用電荷阻擋層降低元件暗電流，能改善有機光偵測器的光偵測度。這些在學術研究上都屬於相當不錯的成果，在期刊與會議論文的發表方面也有不錯的成績，期刊論文已發表了六篇，另有兩篇正在撰寫中，同時我們也有一個專利在申請中。此外，本計劃也培育了數位博士與碩士研究生，在短短一年中有這些成果，整體來看本計劃的執行成效應該非常不錯。

國科會補助專題研究計畫項下出席國際學術會議心得報告

<div align="right">日期：<u>100</u> 年 <u>10</u> 月 <u>26</u> 日</div>

計畫編號	NSC　99－2221－E－009－181－		
計畫名稱	有機光電流增益現象之探討與其在光偵測器的應用		
出國人員姓名	陳方中	服務機構及職稱	交通大學光電工程學系與顯示科技研究所副教授
會議時間	2010 年 12 月 1 日至 2010 年 12 月 3 日	會議地點	日本福岡
會議名稱	（中文）第十七屆國際顯示研討會 （英文）The 17th International Display Workshop (IDW'10)		
發表論文題目	（中文）可撓性有機電晶體於應力狀態下的電性探討 （英文）Electrical Characteristics of Flexible Organic Thin-film Transistors under Bending Conditions		

一、參加會議經過

　　本人於十二月一日早上搭乘飛機至福岡國際機場，於台灣時間十二月四日回國。

　　IDW 算是在日本有關顯示器相關研究技術最重要的國際會議之一，尤其是有不少與有機發光二極體及有機薄膜電晶體元件與面板等最新的技術與進展發表，因此頗受國際重視。酸然此研討會的論文些微偏向應用面，但收集這些相關資料對本研究室的研究課題(有機光電與電子元件)趨勢的掌握相當有助益。而主持人主要參加的為與有機元件有關的 Active Matrix Display(AMD)、Organic LED Display(OLED)及 Flexible Display(FLX)等 workshops。

　　這次會議我在第三天(Dec. 3rd)早上有壁報論文，題目是有關於可撓性有機薄膜電晶體在不同撓曲曲率下的電性分析，過程十分順利，有不少人提了問題，交換了許多意見跟心得。

圖一、會議地點福岡國際會議廳。
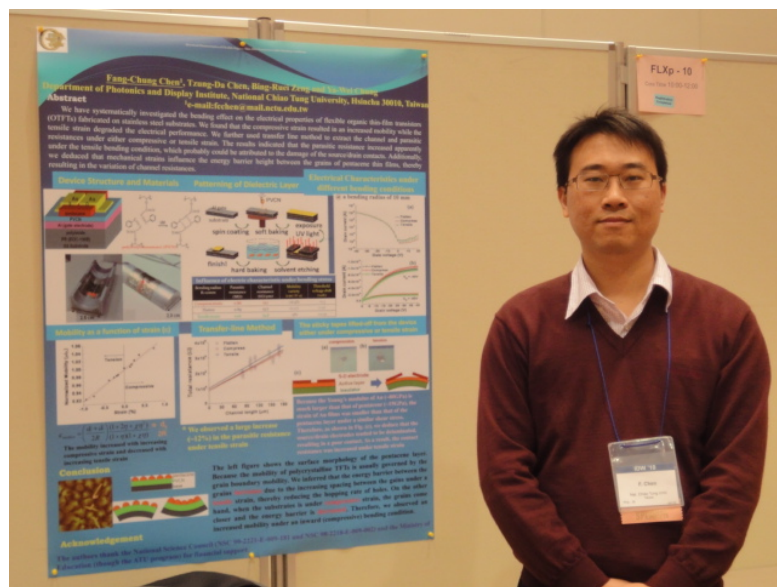
圖二、主持人發表壁報論文。

二、與會心得

　　本次參加此會議的目的，在於發表自己最近的研究成果與收集相關研究的資料，同時也希望能多與國外學者交換研究心得。同時本次參加此國際會議已在短時間內瞭解了許多最新的研究成果，也對國際間的未來研究發展方向有進一步的體認，可謂不虛此行。

　　本次會議聽到了幾個覺得蠻有趣的題目，例如 Dr. K. Yase (AIST, Japan)利用 microcontact printing(μ-CP)在 A4 大小的軟性基板上製作了 200ppi 的 OTFT array，相較於一般的 ink-jet printing 等技術，μ-CP 在控制縱向截面(cross-section)的形狀具有優勢。SONY 繼去年發表的 flexible OTFT-driven OLED Display 後，這次也發表了非常穩定的 OTFT-OLED 軟性面板，此次有機半導體為新穎的 PXX，製成的面板有非常好的均勻性，而作者特別將面板厚度減至 80μm，因此在撓曲半徑非常小的條件下(4 mm)，也有非常好的撓曲特性，以此優良的結果來看，量產可撓性 OTFT-OLED

面板已指日可待。此外，來自 Osaka Pref. University 的 Prof. H, Naito 也發表有機與無機混合材料製作的可撓性 OTFTs，其中絕緣層材料為氧化矽烷為基礎所發展的材料，半導體材料則在 P3HT 中加入氧化矽奈米顆粒，使得兩種材料之間有較好的接面，此可撓性 OTFT 有不錯的元件特性。在氧化物 TFT 方面，AUO 發表利用六代線製作的 backplane，SONY 也發表了修飾絕緣層的改善方法，同時也利用一個新的氧化物 ITZO，比 IGZO 以更好的 mobility，整體看來氧化物的發展也來勢洶洶，都有不錯的元件表現。

三、建議

在福岡期間內也發現一些日本節能減炭的方式，值得我們思考。例如大會不再每位參與者都發十分厚重紙本的論文集，而只有 CD，若要紙本則需額外付費。公車在停紅燈時都會熄火，快變綠燈前才啟動車子。

四、攜回資料名稱及內容

1. Abstracts of the 17th International Display Workshop (IDW'10); 刊載會議發表論文之所有摘要。
2. Proceedings of the 17th International Display Workshop (IDW'10) (CD)

五、其它

感謝國科會於參加經費上之補助，提供在國外發表成果的機會，希望以後能持續補助參加國際會議，除了可多認識外國學者，拓展學術交流網絡，同時也能提高我國研究的能見度。

Paper Title

Electrical Characteristics of Flexible Organic Thin-film Transistors under Bending Conditions

Fang-Chung Chen[*], Tzung-Da Chen

Department of Photonics and Display Institute, National Chiao Tung University, Taiwan

Abstract

The electrical properties of flexible organic thin-film transistors fabricated on stainless steel substrates were measured under different bending conditions. We found that the compressive strain resulted in an increased mobility while the tensile strain leaded to a decreased mobility. From the analysis of the resistances, we deduced that the mechanical strains influence the barrier height between the grains of pentacene thin-films, thereby resulting in the variation of device mobilities.

Presentation Style Preference

Poster Only

Workshop / Topical Session Preference

FLX; Workshop on flexible display

Technical Summary

1. Background and objectives

Organic thin-film transistors (OTFTs) have been received much attention recently because of their potential applications on low-cost, light-weight, and large-area electronic products.[1] More importantly, the mechanical flexibility of organic materials facilitates the preparation of organic devices using high-throughput processes, such as roll-to-roll processing, on flexible substrates. On the other hand, although flexible OTFTs have been widely reported,[2,3] the analysis of electrical properties under bending conditions is still rare.[4,5] In this work, with the use of pentacene as the semiconducting material, and poly(vinyl cinnamate) (PVCN)[6] as the insulator, we fabricated flexible OTFTs on stainless steel (SS) substrates. We found that the compressive strain resulted in an increased mobility while the tensile strain leaded to a decreased mobility. We deduced that the compressive strain forced the grains to become more compact, thereby facilitating the charge transporting between the grains. On the other hand, the tensile strain caused an increase in the spacing between the grains, thereby increasing the barrier height for charge hopping.

2. Results

The device structure is illustrated in Fig. 1 and the material used for each layer is summarized in the inserted table. To fabricate flexible OTFTs on SS substrates, a thick photoresist (EOC-130B) layer was first spin-coated to planarize the surface of the SS foils. Subsequently, a layer of polyimide was also fabricated to modify the surface energy for improving the adhesion of the upper layers on the substrate. Then, Al was thermally evaporated as the gate electrode. For the dielectric layer, poly(vinyl cinnamate) (PVCN) was firstly dissolved in dichlorobenzene (15wt%) and was spin coated on the SS substrates. After a drying process at 80 °C for 10min, the substrate was under UV irradiated (λ=264nm) to crosslink the PVCN (Fig. 1). The substrate was then etched by an organic solvent to define the insulating area. After the etching process, the substrate was dried at 80 °C for 10 min. The thickness of the resulting PVCN layer was ~400 nm. The capacitance was 6.12×10^{-9} F/cm^2. For the active layer, pentacene was thermally deposited (80nm). Finally, Au electrodes were evaporated and served as the source/drain electrodes. We used a shadow mask to define channel length (*L*) and width (*W*). All W/L ratio was 20. The electrical characteristics were measure by Keithley 4200 under atmosphere environment. For the bending tests, the devices were stressed with a bending radius of 10 mm (Figure 2). The bending direction was parallel to that of charge transport.

Figure 3 shows the device output characterization obtained under different mechanical bending conditions. We can clearly see that the drain current increased under compress strain. On the other hand, the current decreased under tensile condition. Further, the current differences increased with the gate voltage. From the above electrical characterization, the device field-effect mobilities were calculated and summarized in Figure 4. The device mobility increased with the channel length.

The device resistance (R_{on}) mainly comes from two contributions: bulk resistance of the semiconductor ($R_{channel}$) and the contact resistance at the interface between the source/drain electrode and the semiconductor ($R_{contact}$). In order to further clarify the effect of mechanical bending, transfer line method (TLM)[7] was adapted to estimate the contact and channel resistances following the equations

$$R_{on} = \partial V_{DS}/\partial I_D \ (V_G\text{=constant}\ ;\ V_{DS} \rightarrow 0) \qquad (1)$$

$$R_{on} = R_{contact} + R_{channel} \qquad (2)$$

$$R_{channel} = L/[WC_i(V_G-V_t)] \quad (3)$$

R_{on} was calculated from the I_d-V_d curves (Figure 3). The TLM results are plotted in Figure 5. The intercept of the curves with y-axis indicated the contact resistance. After knowing the contact resistance, the channel resistance could be also deduced. From the figure, we can see that the major effect of mechanical bending came from the change of channel resistance. The contact resistance remained almost unchanged after bending.

Figure 6 shows the morphology of the pentacene layer, which exhibited polycrystalline morphology. For a polycrystalline TFT, the mobility is usually governed by the grain boundary mobility.[8] In other words, the hopping process is usually limited by the activation energy barrier between the grains. Following this assumption, we propose a model to explain the above observation as the followings. Under a tensile strain [Fig. 6(c)], because the spacing between the gains probably will become longer, the energy barrier between the grains is increased, thereby reducing the hopping rate of holes. On the other hand, when the substrates is under compressive strain, the grains come closer and, subsequently, the energy barrier is decreased [Fig. 6(d)]. Therefore, we observed an increased mobility under an inward bending condition.

3. Originality

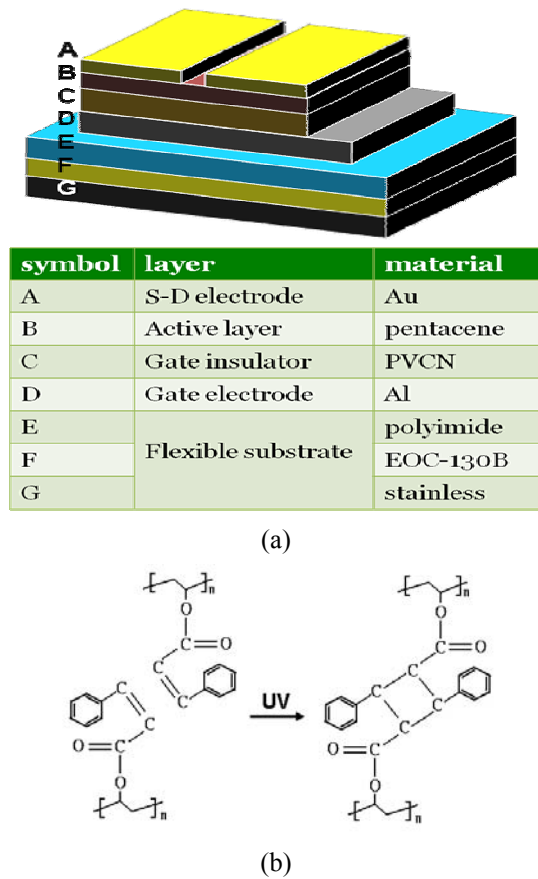The data presented is original.

4. Impact

This study studies the effect of mechanical strain on the pentacene-based organic thin film transistors. The OTFTs were fabricated on flexible stainless steel (SS) substrates and measured under different bending conditions. We observed that the compressive strain resulted in an increased mobility while the tensile strain leaded to a decreased mobility. We further used transfer line method to extract the channel and parasitic resistances, and found that the major impact of the mechanical bending was on the channel resistance. We suspected that mechanical strains influence the barrier height between the grains of pentacene thin-films, thereby resulting in the variation of device mobilities.

5. Reference

1. J. Zaumseil and H. Sirringhaus, Chem. Rev. **107**, 1296 (2007).

2. L. Zhou, A. Wanga, S. C. Wu, J. Sun, S. Park, and T. N. Jackson, Appl. Phys. Lett. **88**, 083502 (2006).

3. X. H. Zhang, W. J. Potscavage, Jr., S. Choi, and B. Kippele, Appl. Phys. Lett. **94**, 043312 (2009).

4. T. Sekitani, Y. Kato, S. Iba, H. Shinaoka, T. Someya, T. Sakurai, and S. Takagi, Appl. Phys. Lett. **86**, 073511 (2005).

5. Y. G. Seol, H. Y. Noh, S. S. Lee, J. H. Ahn, and N. E. Lee, Appl. Phys. Lett. **93**, 013305 (2008).

6. J. Jang, S. H. Kim, S. Nam, D. S. Chung, C. Yang, W. M. Yun, C. E. Park, and J. B. Koo, Appl. Phys. Lett. **92**, 143306 (2008).

7. S. Sherman, P. Y. Lu, R. A. Gottscho, and S. Wagner, Mater. Res. Soc. Symp. Proc. **377**, 749 (1995).

8. G. Horowitz, Adv. Funct. Mat. **13**, 53 (2003).

6. Prior publications

No

symbol	layer	material
A	S-D electrode	Au
B	Active layer	pentacene
C	Gate insulator	PVCN
D	Gate electrode	Al
E	Flexible substrate	polyimide
F		EOC-130B
G		stainless

(a)

(b)

Fig. 1 The device structure and materials used in this study. (b)The chemical structure of PVCN and the photo-crosslinking reaction.
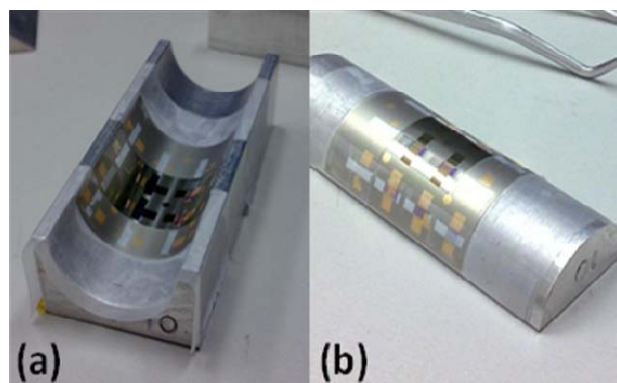
Fig. 2 The schematic presentation of the bending test apparatus: (a) compressive (inward) and (b) tensile (outward) bending. The bending direction was parallel to the channel.

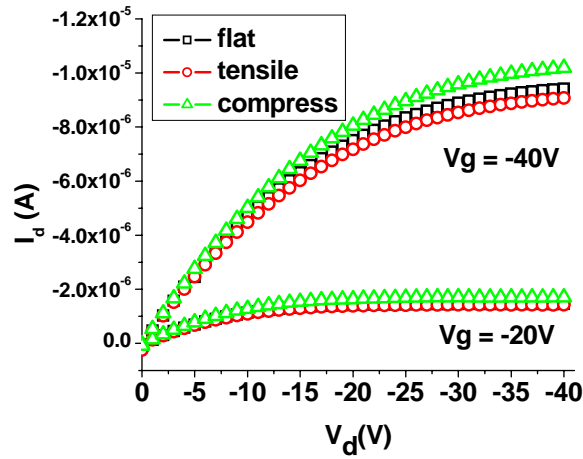**Fig. 3 The output characteristics of the device measured under compressive and tensile strains (L=160μm, W=0.2cm).**

Fig. 4 The mobility of the OTFTs under different mechanical strains as a function of channel length (V_D=-40V).

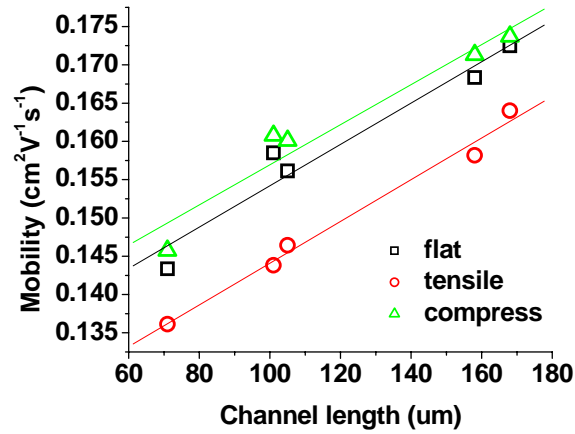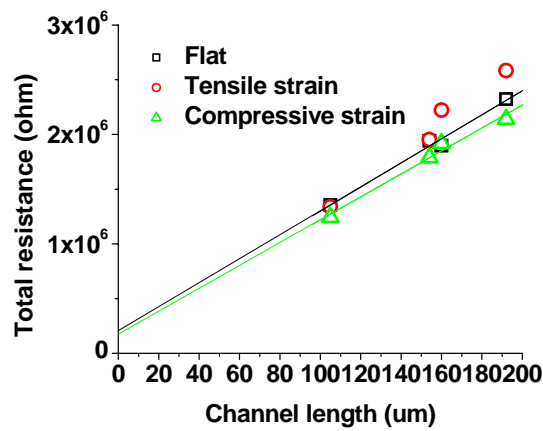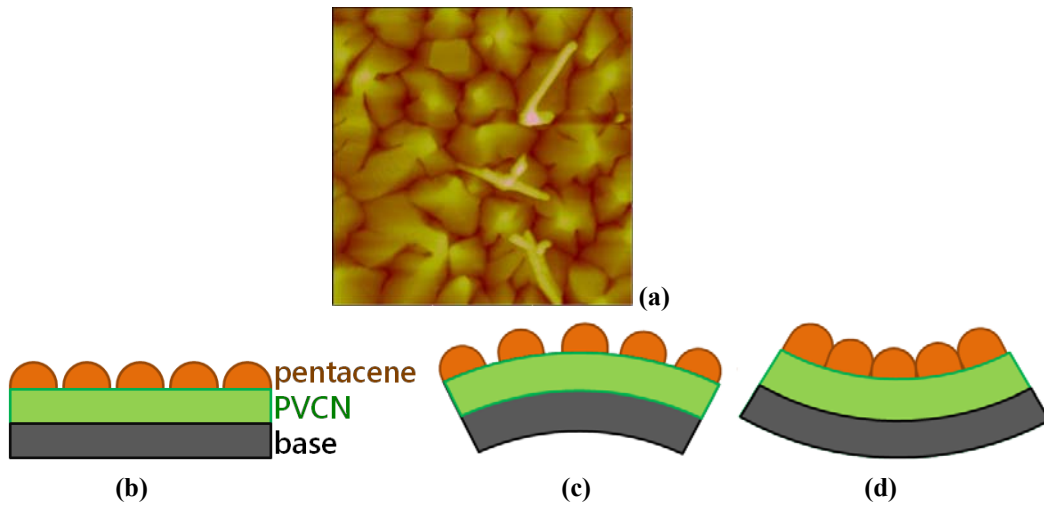**Fig. 5 The mobility of the OTFTs under different mechanical strains as a function of channel length (V_D=-40V).**

Fig. 6 (a)The surface morphology of the pentacene layer. The schematic representation of the gains of the pentacene layer on a (b) flat substrate; (c) substrate under tensile strain; (d) substrate under compressive strain.

國科會補助專題研究計畫項下出席國際學術會議心得報告

<div align="right">日期：<u>100</u> 年 <u>10</u> 月 <u>24</u> 日</div>

計畫編號	NSC　99－2221－E－009－181－
計畫名稱	有機光電流增益現象之探討與其在光偵測器的應用

出國人員 姓名	陳方中	服務機構 及職稱	交通大學光電工程學系與顯示科 技研究所副教授
會議時間	2010 年 12 月 3 日 至 2010 年 12 月 6 日	會議地點	大陸廣州

會議名稱	（中文）先進光電子學及微奈米光學研討會 （英文）IEEE/OSA Advanced in Optoelectronics and Micro/nano-optics
發表論文 題目	（中文）高效能高分子太陽能電池的集光結構設計 （英文）Light Harvesting Schemes for High-performance Polymer Solar Cells

一、參加會議經過

　　此次會議是 IEEE 及 OSA 在區域性舉辦的專題性研討會，而除了邀請演講的口頭報告之外，很榮幸的是也能在此會議中擔任國際議程規劃委員(International Technical Program Committee)。這次會議我的演講被安排在第三天(Dec. 5th)下午，題目是有關於高分子太陽能電池的集光結構設計，演講過程十分順利，也有聽眾提了問題。此外，在會議其間內也遇到了不少同行的研究學者，例如來自現今高分子太陽能電池業界位居領導地位的 Solamer 的李剛(Gang Li)博士，及大陸中科院的李永舫(Yongfang Li)教授及不少從香港新加坡等地來的學者，也與這些同行交換了許多意見跟心得。此外，較特別的是大會也在第三天晚上安排夜遊珠江的活動，也更加多了交流的機會。

二、與會心得

　　本次參加此會議除了發表自己最近的研究成果與收集相關研究的資料，同時也希望能多與國外學者交換研究心得。特別是從美國 Solarmer 來的李博士，因有第一手的研究資訊，更能及時了解目前最先進的研究成果。

此外，此次是主持人第一次到廣州，發現廣州的硬體設備目前看來已完全不輸台灣的大城市了，特別是在舉辦亞運之後，城市面貌改變許多，但仔細來看，軟體方面如人文素質等台灣還是略有優勢，因此台灣不應再迷信大資本而想短期間內可回收的硬體投資，而應更加強軟性方面的投資，多扎根基本科學的研發，才有辦法長遠的發展下去。

三、建議

　　台灣應多爭取國際會議的舉辦機會，如本次會議大會安排的珠江夜遊的活動，另人印象深刻，也成功達成國際城市行銷的目的，可謂一舉數得。

四、攜回資料名稱及內容

1.　Technical Program of Advanced in Optoelectronics and Micro/nano-optics; 刊載會議發表論文之所有演講摘要與時程。

五、其它

　　感謝國科會於參加經費上之補助，提供發表研究成果的機會，除了可多拓展學術交流網絡，同時也能提高我國研究的能見度。

Light Harvesting Schemes for High-performance Polymer Solar Cells

Fang-Chung Chen, Yi Hung
Department of Photonics and Display Institute
National Chiao Tung University
Hsinchu, Taiwan
fcchen@mail.nctu.edu.tw

Juh-Lih Wu
Institute of Electro-optical Engineering
National Chiao Tung University
Hsinchu, Taiwan

Abstract—**In this paper, we will present approaches for light harvesting for enhancing the performance of polymer solar cells. We have employed indium tin oxide (ITO) as an optical spacer in inverted structures. We have found that the optical interference effect led to spatial redistribution of the optical field in the devices, resulting in favorable distribution of photogenerated excitons. Therefore, the introduction of the ITO optical spacer at an appropriate thickness increased the short-circuit current density and the overall power conversion efficiency.**

Keywords-Polymer; solar cell; light trapping; optical

I. INTRODUCTION

Recently organic photovoltaic devices (OPVs) have received widely attention because they could offer low-cost, low temperature approaches, such as roll-to-roll and printing methods, for the manufacture of cheap energy sources. Furthermore, these devices potentially could be also applied onto portable electronics devices due to their light-weight and mechanical flexibility [1-3]. One of the key issues toward achieving high efficiency is sufficient photo-absorption. To use a thicker active layer to increase the absorption, however, inevitably leads to a larger device series resistance, due to the much lower motilities of organic materials. Therefore, it is of importance to develop effective methods for efficient sunlight harvesting through light trapping technology without sacrifice of the electrical properties.

In this paper, we will present the light trapping scheme for enhancing the power conversion efficiency (PCE) of polymer solar cells. We incorporated a layer of indium tin oxide (ITO) as an optical spacer in inverted OPV devices. ITO appears to be a suitable candidate for use as a functional optical spacer between the organic active layer(s) and the electrode in the OPVs because of its high electrical conductivity (to avoid the increased device resistance) and high optical transparency. However, its work function somehow misaligns with the highest occupied molecular orbital of the *p*-type conducting polymer, which might result in a high contact resistance. This problem could be easily solved, however, by incorporating molybdenum trioxide (MoO_3) as an interlayer to match the energy levels. Our experimental and theoretical studies of this MoO_3/ITO "bilayer structure" revealed that the introduction of the ITO optical spacer notably enhanced the exciton generation rate, thereby increasing both the photocurrent and the overall device efficiency. More interestingly, the optical interference effect, induced by the presence of the ITO optical spacer, remained beneficial to the device performance of inverted OPVs when optimizing the thickness of the active layer.

II. EXPERIMENTAL

Fig. 1 provides a schematic representation of the devices' structural configuration. To fabricate inverted OPVs, an interfacial layer of cesium carbonate (Cs_2CO_3) was spin-coated onto the ITO-coated (thickness: 180 nm) glass substrate, followed by thermal annealing at 150 °C for 15 min. The work function of the resulting ITO layer was reduced to 3.4 eV, facilitating electron collection at the cathode [4]. The photoactive layer was spin-coated on top of the Cs_2CO_3 from a blend (1:1,w/w) of poly(3-hexylthiophene) (P3HT) and [6,6]-phenyl-C_{61}-butyric acid methyl ester (PCBM) dissolved in 1,2-dichlorobenzene (DCB). After solvent annealing [1], the dried film was thermally annealed at 110 °C for 15 min; the resulting film was ca. 180 nm thick. To complete the device, 20 nm–thick MoO_3 and 150 nm–thick Ag layers were sequentially deposited through thermal evaporation to function as the hole-collection contact. Here, Ag was used as the anodic electrode because of its high reflectance and conductivity. ITO layers of various thicknesses (50, 100, and 150 nm) were inserted between the MoO_3 and Ag layers through rf sputtering to function as optical spacers. The device area, defined through a shadow mask, was 0.12 cm^2. All of the completed devices were thermally post-annealed at 140 °C for 5 min in a glove box. The current density–voltage (J–V) characteristics of the devices were measured using a Keithley 2400 source-measure unit. The photocurrent was obtained under air mass 1.5 global (AM 1.5G) illumination from a 150 W Thermal Oriel solar simulator. The illumination intensity was calibrated using a standard Si photodiode equipped with a KG-5 filter (Hamamatsu, Inc.) [5]. Optical modeling was performed using the optical transfer matrix formalism (TMF) approach [6]. The optical constants, including the refractive index (n) and extinction coefficient (k), of each layer in the device structure were obtained using the ellipsometry method. The film thickness of each layer was determined using atomic force microscopy (AFM) and ellipsometry measurements.
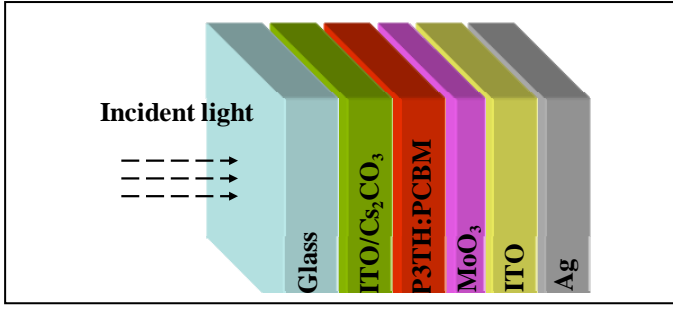
Figure 1. Schematic representation of the device architecture of OPVs incorporating an ITO optical spacer.

III. RESULTS AND DISSCUSSION

Fig. 2 displays the *J–V* characteristics, recorded under 100 mW cm^{-2} illumination, of OPV devices incorporating ITO optical spacers of various thicknesses. The reference device possessing the structure ITO/Cs$_2$CO$_3$/P3HT:PCBM/MoO$_3$/Ag exhibited an open-circuit voltage (V_{oc}) of 0.59 V, a short-circuit current (J_{sc}) of 9.54 mA cm^{-2}, and a fill factor (FF) of 0.67, yielding an overall device PCE of 3.76%. The typical photovoltaic characteristics suggested that functional contacts were formed at both contacts (ITO/Cs$_2$CO$_3$ and MoO$_3$/Ag). Note that Cs$_2$CO$_3$ [4] and MoO$_3$ [7] have been proposed to act as functional electron- and hole-selective layers, respectively, for efficient charge collection in OPVs.
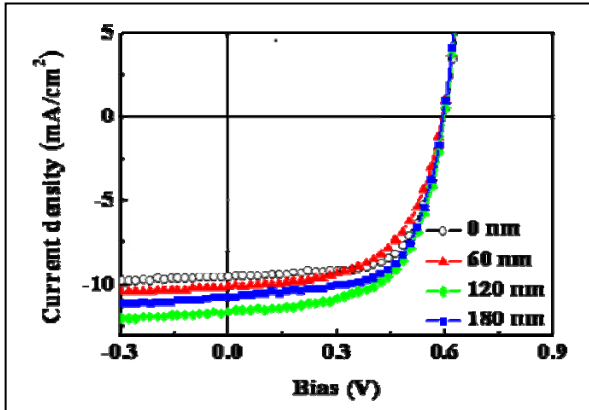

Figure 2. *J–V* characteristics, recorded under 100 mW cm^{-2} illumination (AM 1.5G), of polymer solar cells incorporating ITO optical spacers of various thicknesses.

To further benefit from the optical interference effect, we inserted ITO layers of various thicknesses (60, 120, and 180 nm) between the MoO$_3$ and Ag layers. In each case, the value of V_{oc} remained at 0.59 V. In contrast, the value of J_{sc} was strongly dependent on the ITO thickness: its optimum value occurred for an ITO thickness of 120 nm. Moreover, the FF decreased slightly after inserting the ITO optical spacers, presumably because of increased device series resistance arising from the presence of ITO [8] and/or possible sputtering damage. Such problems could, however, be overcome through the incorporation of an optical spacer of a suitable thickness.

The device incorporating the 120 nm–thick ITO optical spacer achieved an excellent PCE of 4.20% (V_{oc} = 0.59 V; J_{sc} = 11.49 mA cm^{-2}; FF = 0.62). In general, the expected benefit from the optical interference effect is negated when the active layer is sufficiently thick [9]. Amazingly, the inverted OPVs fabricated in this study could still benefit from the introduction of an ITO optical spacer when the thickness of the active layer was optimized.

Fig. 3 compares the incident photon–to–electron conversion efficiency (IPCE) curves for devices with and without optical spacers. The IPCE, the ratio of the number of collected electrons to that of absorbed photons, is measured to determine the spectral response of OPVs; it is given by

$$IPCE(\%) = 1240 \times \frac{J_{sc}}{\lambda \times I_\lambda} \times 100\% \tag{1}$$

where λ is the wavelength and I_λ is the incident light intensity from the monochromatic light source. Fig. 3 reveals that the spectral response changed significantly after inserting an ITO optical spacer, presumably because of the interference effect caused by the ITO optical spacer.

Figure 3. IPCE curves of polymer solar cells incorporating ITO optical
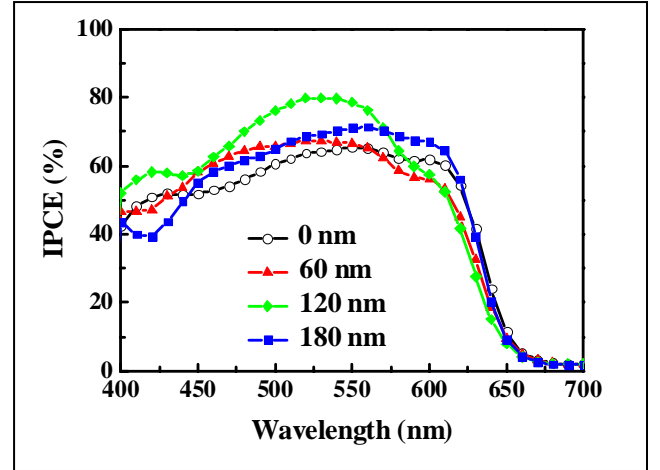
spacers of various thicknesses.

To further study the mechanism responsible for the increased photocurrent, we also numerically investigated the optical interference effect of incorporating an optical spacer in OPVs through TMF optical modeling, which has been used widely to investigate the optical behavior of OPV devices [9,10]. The optical field intensity ($|E(z)|^2$) at any given position in the device can be calculated from the optical constants (*n* and *k*) and the depth of each layer. Figure 4 displays the effect of the optical spacers on the calculated distribution profiles of optical field intensity in the device at given wavelengths (λ) of 500 and 550 nm. The spatial distribution of the optical field intensity was strongly dependent on the thickness of the optical space.

For quantitative analysis, therefore, we further calculated the distribution profiles for the exciton generation rate $G(z)$ inside the active layer via the energy dissipation rate (Fig. 5) [11]. Figure 5 reveals that the incorporation of an ITO spacer effectively tailored the distribution of photo-generated excitons. After incorporating a 120 nm–thick ITO optical spacer, the values of $G(z)$ increased within the depth range from 60 to 120 nm but decreased near both organic/electrode contacts. We suspect that the dramatic change in the distribution profile of $G(z)$ contributed to the enhanced photocurrent.
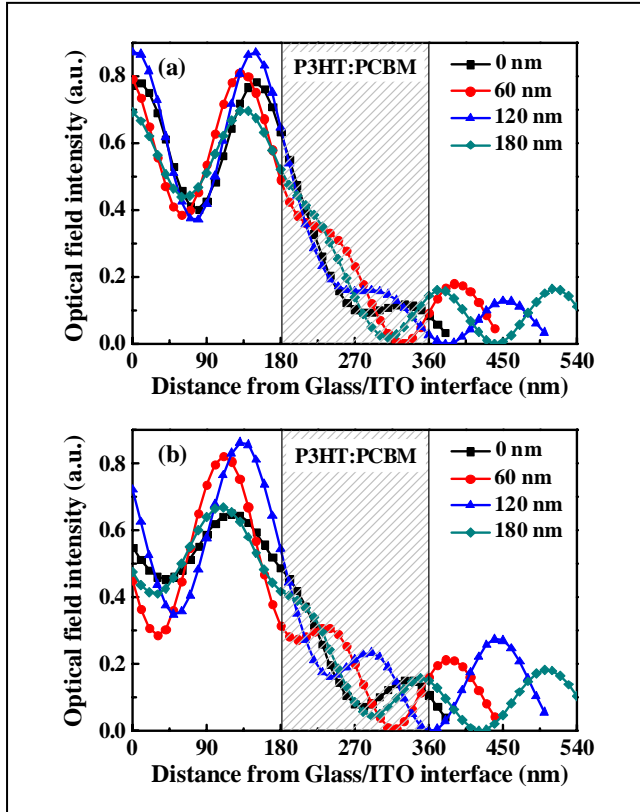

Figure 4. Calculated distribution profiles for the optical field intensities in OPV devices incorporating ITO optical spacers of various thicknesses, determined at wavelengths of (a) 500 and (b) 550 nm.

Previously, Moulé and Meerholz suggested that the photocurrent decreased when the light intensity in the proximity of the organic/electrode interface increased due to the exciton quenching (recombination) in conventional devices [12]. In the present study, the shift of the exciton generation zone away from the electrodes probably diminished possible exciton quenching at the electrodes. Therefore, the use of an ITO optical spacer of an appropriate thickness can give rise to a favorable distribution profile of $G(z)$ for maximizing the number of "effective" photon-generated excitons. Finally, we note that the "optical spacers" failed to increase the amount of excitons (which can be calculated by integrating the area beneath the curves in Fig. 5) because our devices had sufficiently thick films for photon harvesting. However, the favorable distribution profile of $G(z)$ was still beneficial for improving the overall device efficiency of OPVs.
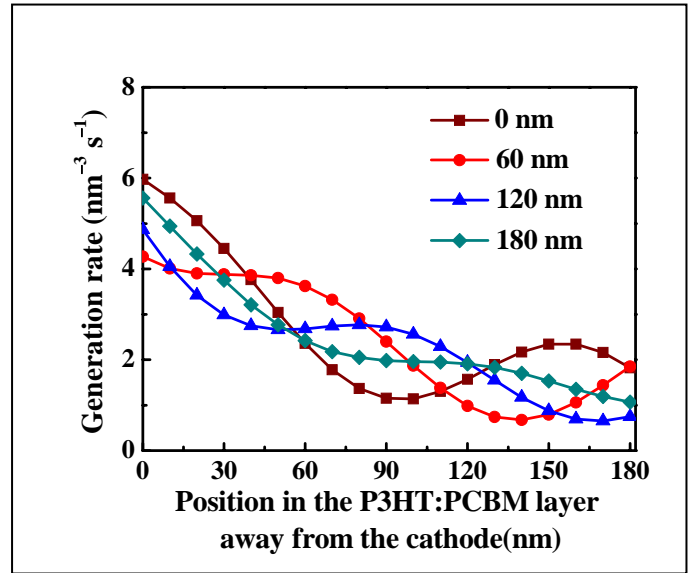

Figure 5. Calculated distribution profiles of the exciton generation rate inside the active layer for OPV devices incorporating ITO optical spacers of various thicknesses. Inset: Schematic illustration of our layer stack.

IV. CONCLUSION

Efficient light absorption in thin film solar cells is critical to improving their performance—especially for those based on organic materials, where the thickness of the active layer is typically ca. 200 nm. We have improved the PCE of the inverted OPVs by incorporating an ITO optical spacer, thereby achieving interference-enhanced devices. The resulting optical interference effect led to spatial redistribution of the optical field intensity and the distribution profile of exciton generation rate. Although the degree of light absorption in inverted OPVs was not increased, the resulting favorable distribution of photo-generated excitons probably decreased the level of exciton quenching near the electrodes. Our results indicate that the inverted OPVs could still benefit from such optical effects when they had a sufficiently thick active layer.

REFERENCES

[1] G. Li, V. Shrotriya, J. S. Huang, Y. Yao, T. Moriarty, K. Emery, and Y. Yang, "High-performance solution processable polymer photovoltaic cells by self-organization of polymer blends," Nat. Mater., vol. 4, pp. 864-868, Nov. 2005.

[2] J. Peet, Mi. L. Senatore, A. J. Heeger, and G. C. Bazan, "The role of processing in the fabrication and optimization of plastic solar cells," Adv. Mater., vol. 21, pp. 1521-1527, April 2009.

[3] F. C. Krebs, J. Fyenbo and M. Jørgensen, "Product integration of compact roll-to-roll processed polymer solar cell modules: methods and manufacture using flexographic printing, slot-die coating and rotary screen printing," J. Mater. Chem., in press.

[4] H. H. Liao, L. M. Chen, Z. Xu, G. Li and Y. Yang, "Highly efficient inverted polymer solar cell by low temperature annealing of Cs_2CO_3 interlayer," Appl. Phys. Lett., vol. 92, pp. 173303-1-173303-3, April 2008.

[5] V. Shrotriya, G. Li, Y. Yao, T. Moriarty, K. Emery and Y. Yang, "Accurate measurement and characterization of organic solar cells," Adv. Funct. Mater., vol. 16, pp. 2016–2023, Oct. 2006.

[6] L. A. A. Pettersson, L. S. Roman and O. Inganas, "Modeling photocurrent action spectra of photovoltaic devices based on organic thin films," J. Appl. Phys., vol. 86, pp. 487–496, July 1999.

[7] C. Tao, S. P. Ruan, X. D. Zhang, G. H. Xie, L. Shen, X. Z. Kong, W. Dong, C. X. Liu and W. Y. Chen, "Performance improvement of inverted polymer solar cells with different top electrodes by introducing a MoO_3 buffer layer," Appl. Phys. Lett., vol. 93, pp. 193307-1-193307-3, Nov. 2008.

[8] K. Kawano, N. Ito, T. Nishimori and J. Sakai, "Open circuit voltage of stacked bulk heterojunction organic solar cells," Appl. Phys. Lett. vol. 88, pp. 073514-1-073515-3, Feb. 2006.

[9] J. Gilot, I. Barbu, M. M. Wienk and R. A. J. Janssen, "The use of ZnO as optical spacer in polymer solar cells: Theoretical and experimental study," Appl. Phys. Lett., vol. 91, pp. 113520-1-113520-3, Sep. 2007.

[10] A. Roy, S. H. Park, S. Cowan, M. H. Tong, S. N. Cho, K. Lee and A. J. Heeger, "Titanium suboxide as an optical spacer in polymer solar cells," Appl. Phys. Lett. vol. 95, pp. 013302-1-013302-3, July 2009

[11] C. F. Zhang, S. W. Tong, C. Y. Jiang, E. T. Kang, D. S. H. Chan and C. X. Zhu, "Efficient multilayer organic solar cells using the optical interference peak," Appl. Phys. Lett., vol. 93, pp. 043307-1-043307-3, July 2008.

[12] A. J. Moulé and K. Meerholz, "Intensity-dependent photocurrent generation at the anode in bulk-heterojunction solar cells," Appl. Phys. B-Lasers Opt., vol. 92, pp. 209-218, 2008.

國科會補助計畫衍生研發成果推廣資料表

國科會補助計畫	計畫名稱: 有機光電流增益現象之探討與其在光偵測器的應用		
	計畫主持人: 陳方中		
	計畫編號: 99-2221-E-009-181- 　　　　學門領域: 光電子材料元件與模組		
研發成果名稱	（中文）以電荷阻擋層提升光增益有機光偵測器之偵測度		
	（英文）Using charge blocking layers for improving detectivities of organic photomultiple photodetectors		
成果歸屬機構	國立交通大學	發明人 （創作人）	陳方中,林書丞
技術說明	（中文）有機光偵測器已有不少的相關文獻，如早在1994年，A. J. Heeger等人在高分子材料中加入C60之後，發現可以大幅增加元件敏感度。但利用光子增益現象的有機光偵測器並不多見，如在2008年，H. Y. Chen等人於Nature Nanotechnology中發表了一篇關於光子增益(Photomultiplication)現象的論文，此光偵測器確實能偵測到更寬廣的波長範圍，也有更高的靈敏度。而在2010年，本研究室則利用摻雜有機近紅外光染料的簡易方式製作具有非常高光敏感度的光偵測器。另一方面，在2011年，G. Sarasqueta等人則利用有機及無機的阻擋層(blocking layer)降低有機無機混成光感測元件的暗電流，藉以提升元件的偵測度(detectivity)。本案利用加入電荷阻擋層的方式降低有機光增益偵測器的暗電流，在逆向偏壓-4V下，暗電流可從偵測度-43.8降低至-1.82 mA/cm2。同時因為較低的暗電流，有機光增益偵測器的偵測度也可大幅改善。		
	（英文）We have found the incorporation of charge blocking layer could effectively suppress the dark current of organic photomultiple photodetectors. The dark current was reduced from -43.8 mA/cm2 to 1.82 mA/cm2 while the bias voltage was -4V. Due to the reduction of the dark current, the detectivity has been improved substantially.		
產業別	機電工程業；光學及精密器械製造業；電機及電子機械器材業		
技術/產品應用範圍	光偵測器，煙霧偵測器，功率計，光學觸控板，夜視鏡等		
技術移轉可行性及預期效益	如本案之技術能成功商品化，會有相當高靈敏度的光偵測器，並且偵測的波長相當廣，預估將是市場上相關產品最具有潛力者。		

註：本項研發成果若尚未申請專利，請勿揭露可申請專利之主要內容。

99 年度專題研究計畫研究成果彙整表

計畫主持人：陳方中　　　　計畫編號：99-2221-E-009-181-

計畫名稱：有機光電流增益現象之探討與其在光偵測器的應用

成果項目			量化			單位	備註（質化說明：如數個計畫共同成果、成果列為該期刊之封面故事...等）
			實際已達成數（被接受或已發表）	預期總達成數(含實際已達成數)	本計畫實際貢獻百分比		
國內	論文著作	期刊論文	2	2	50%	篇	兩個計畫共同成果
		研究報告/技術報告	0	0	100%		
		研討會論文	4	4	100%		一篇已發表於 IDMC 2011 另三篇將發表於 IPC 2011(光電學門成果發表會及研討會)
		專書	0	0	100%		
	專利	申請中件數	1	1	100%	件	
		已獲得件數	0	0	100%		
	技術移轉	件數	0	0	100%	件	
		權利金	0	0	100%	千元	
	參與計畫人力（本國籍）	碩士生	4	2	100%	人次	兩個計畫共同成果
		博士生	2	1	50%		
		博士後研究員	0	0	100%		
		專任助理	0	0	100%		
國外	論文著作	期刊論文	6	2	70%	篇	若干為兩個計畫共同成果
		研究報告/技術報告	0	0	100%		
		研討會論文	3	2	80%		其中一篇為兩個計畫的共同成果
		專書	0	0	100%	章/本	
	專利	申請中件數	1	1	100%	件	
		已獲得件數	0	0	100%		
	技術移轉	件數	0	0	100%	件	
		權利金	0	0	100%	千元	
	參與計畫人力（外國籍）	碩士生	0	0	100%	人次	
		博士生	0	0	100%		
		博士後研究員	0	0	100%		
		專任助理	0	0	100%		

	成果項目	量化	名稱或內容性質簡述
其他成果 (無法以量化表達之成果如辦理學術活動、獲得獎項、重要國際合作、研究成果國際影響力及其他協助產業技術發展之具體效益事項等,請以文字敘述填列。)	無		

	成果項目	量化	名稱或內容性質簡述
科教處計畫加填項目	測驗工具(含質性與量性)	0	
	課程/模組	0	
	電腦及網路系統或工具	0	
	教材	0	
	舉辦之活動/競賽	0	
	研討會/工作坊	0	
	電子報、網站	0	
	計畫成果推廣之參與（閱聽）人數	0	

國科會補助專題研究計畫成果報告自評表

請就研究內容與原計畫相符程度、達成預期目標情況、研究成果之學術或應用價值（簡要敘述成果所代表之意義、價值、影響或進一步發展之可能性）、是否適合在學術期刊發表或申請專利、主要發現或其他有關價值等，作一綜合評估。

---

1. 請就研究內容與原計畫相符程度、達成預期目標情況作一綜合評估

   ■達成目標

   □未達成目標（請說明，以 100 字為限）

   　　□實驗失敗

   　　□因故實驗中斷

   　　□其他原因

   　說明：

---

2. 研究成果在學術期刊發表或申請專利等情形：

   論文：■已發表　□未發表之文稿　□撰寫中　□無

   專利：□已獲得　■申請中　□無

   技轉：□已技轉　□洽談中　■無

   其他：（以 100 字為限）

   還有兩篇國際期刊未發表

---

3. 請依學術成就、技術創新、社會影響等方面，評估研究成果之學術或應用價值（簡要敘述成果所代表之意義、價值、影響或進一步發展之可能性）（以 500 字為限）

   本計畫已成功證明在主動層摻雜有機染料分子後，可得到明顯的光電增益效應。我們也發現藉由不同的有機染料分子摻雜，可以延伸元件可以偵測的波長。最後，我們也成功利用電荷阻擋層降低元件暗電流，能改善有機光偵測器的光偵測度。這些在學術研究上都屬於相當不錯的成果，在期刊與會議論文的發表方面也有不錯的成績，期刊論文已發表了六篇，另有兩篇正在撰寫中，同時我們也有一個專利在申請中。此外，本計劃也培育了數位博士與碩士研究生，在短短一年中有這些成果，整體來看本計劃的執行成效應該非常不錯。